Development of the next-generation air quality prediction system in the Unified Forecast System framework: Enhancing predictability of wildfire air quality impacts

Jianping Huang[1], Ivanka Stajner[1], Raffaele Montuoro[1], Fanglin Yang[1], Kai Wang[2, 1], Ho-Chun Huang[2, 1], Chan-Hoo Jeon[3, 4], Brian Curtis[2, 1], Jeff McQueen[1], Haixia Liu[2, 1], Barry Baker[5], Daniel Tong[6], Youhua Tang[5, 6], Patrick Campbell[5, 6], Georg Grell[7], Gregory Frost[8], Rebecca Schwantes[8], Siyuan Wang[8, 9], Shobha Kondragunta[10], Fangjun Li[11], and Youngsun Jung[12]

[1] Environmental Modeling Center, NOAA/NWS/NCEP, College Park, MD, USA

[2] Lynker, Leesburg, VA, USA

[3] Earth Prediction Innovation Center, NOAA/OAR/WPO, Silver Spring, MD, USA

[4] Raytheon/STC, Riverdale, MD, USA

[5] Air Resources Laboratory, NOAA/OAR, College Park, MD, USA

[6] Center for Spatial Information Science and Systems, George Mason University, Fairfax, VA, USA

[7] Global System Laboratory, NOAA/OAR, Boulder, CO, USA

[8] Chemical Sciences Laboratory, NOAA/OAR, Boulder, CO, USA

[9] CIRES, University of Colorado Boulder, Boulder, CO, USA

[10] Center for Satellite Applications and Research, NOAA/NESDIS, College Park, MD, USA

[11] South Dakota State University, Brookings, SD, USA

[12] The Office of Science and Technology Integration, NOAA/NWS, Silver Spring, MD, USA

Corresponding authors: Jianping Huang (jianping.huang@noaa.gov) and Ivanka Stajner (ivanka.stajner@noaa.gov)

Early Online Release: This preliminary version has been accepted for publication in *Bulletin of the American Meteorological Society*, may be fully cited, and has been assigned DOI 10.1175/BAMS-D-23-0053.1. The final typeset copyedited article will replace the EOR at the above DOI when it is published.

Abstract

The National Oceanic and Atmospheric Administration (NOAA) has developed an advanced regional air quality prediction system (AQPS) within the Unified Forecast System (UFS) framework to improve representations of wildfire emissions and their impacts on air quality predictions. This innovative system integrates the Environmental Protection Agency's (EPA) Community Multiscale Air Quality (CMAQ) model as a column chemistry model with the UFS-based atmospheric model, operating in an online mode. The calculation of wildfire gas and particulate emissions relies on satellite-derived fire products, high-resolution Regional Hourly Advanced Baseline Imager (ABI) and Visible Infrared Imaging Radiometer Suite (VIIRS) Emissions (RAVE).

A period in June and July 2023 with Quebec Canadian wildfires, which severely impacted air quality in the United States (US), was chosen as a case study to assess the predictive capability of the UFS-AQM system. The UFS-AQM predictions of fine particulate ($PM_{2.5}$) and ozone (O_3) were evaluated against AirNow observations from June 15 to July 14, 2023. The results indicate a substantial improvement in $PM_{2.5}$ predictions when compared to the previous operational forecast. Meanwhile, the system demonstrates a strong ability of predicting O_3 exceedance events during the dissipation phase of the wildfire. Furthermore, the online system shows more realistic predictions of aerosol optical depth (AOD) as compared to the previous operational forecast and satellite retrieval data. Finally, this study outlines a plan for further advancing a comprehensive regional AQPS at NOAA.

Significance Statement

This study marks a historic milestone as NOAA leads the development of an online coupled -air quality prediction system (AQPS) within the Unified Forecast System (UFS) framework. The innovative UFS-AQM online system improves the representation of wildfire emissions and their impacts on air quality predictions. The system shows significant improvements in forecasting fine particulate matter ($PM_{2.5}$) and ozone (O_3) exceedance events compared to the current operational system during wildfire events. The development of the UFS-AQM online system has significantly improved wildfire-

Accepted for publication in *Bulletin of the American Meteorological Society.* DOI 10.1175/BAMS-D-23-0053.1.

driven air quality predictions and will potentially benefit weather forecasting in the near future via improvements of meteorology-chemistry feedbacks in the models.

CAPSULE

NOAA has developed the first online coupled AQPS within the UFS framework to address the air quality prediction challenges imposed by growing wildfires over North America.

Motivation and Objectives

Ozone (O_3) and particulate matter with diameter less than or equal to 2.5 μm ($PM_{2.5}$) are the primary contributors to poor air quality in the United States (US). Exposure to elevated levels of ambient air pollutants has been associated with adverse health effects, particularly for vulnerable populations such as children, the elderly, and individuals with pre-existing respiratory or cardiovascular conditions (e.g., Demetirou and Vineis, 2015; Kar Kurt et al., 2016). Over the past few decades, poor air quality has been responsible for more than 100,000 deaths per year in the US, which is orders-of-magnitude higher than the total fatalities caused by all other weather phenomena, averaging about 500 per year in the US (https://www.weather.gov/hazstat, Fann et al., 2012). Providing accurate and timely forecast guidance is therefore critical to create a basis for alerting vulnerable individuals to avoid or reduce their exposure to poor air quality.

Wildfires pose a significant challenge to air quality prediction. Wildfires account for 15 to 30% of $PM_{2.5}$ emissions in the US (US EPA, 2017), which has significant implications for air quality, human health, and ecosystems (Bowman et al., 2020, Johnston et al., 2012, Burke, et al. 2021, Schill et al., 2020, Xie et al., 2022). While anthropogenic emissions have decreased significantly, wildfires, a significant source of poor air quality, have been on the rise including frequency and intensity in the US over the past few decades (e.g., Xie et al., 2022). There are large uncertainties in wildfire emissions used by the previous operational systems, including fire intensity, speciation, burning duration, diurnal evolution, and smoke plume-rise height (e.g., Andreae, 2019; Chatfield, et al. 2020). For instance, the previous NOAA operational air quality predictions use daily constant satellite-retrieved fire emission products with a one-day latency. Thus, improving the

Accepted for publication in *Bulletin of the American Meteorological Society.* DOI 10.1175/BAMS-D-23-0053.1.

representation of wildfire emissions is essential to enhancing air quality predictions during wildfire events.

Accurate meteorological inputs are another critical factor to improve air quality predictions. In previous air quality prediction systems at NOAA, weather and air quality models (AQM) run separately on disparate grids, with different map projections, transport algorithms, and physical parameterization packages, through an offline-coupling approach (Campbell, et al, 2022). The meteorological fields are updated in the AQM through grid-mapping and vertical coordinate interpolation at a frequency of an hour, rather than each model integration time step. This approach may introduce additional uncertainties in air quality predictions due to grid-mapping, vertical coordinate interpolation, and mismatch between interpolation time frequency and actual model time step (e.g., Bellasio and Foley, 2016). To minimize such uncertainties and enhance the accuracy of air quality predictions, it is crucial to develop an online-coupling system that enables running both weather and air quality models on the same grids and coordinate systems, while utilizing the same transport algorithms and physics packages.

Under funding of the Fiscal Year 2019 Disaster Supplement Program and Disaster Relief Supplemental Appropriations Act 2022, a collaborative effort across NOAA has been dedicated to developing the next generation AQPS for the US within the UFS framework (Jacobs, 2021). This marks the first time that NOAA developed and tested an online-coupling weather and AQPS targeted at operational implementation. The collaborative efforts aim to achieve three objectives: 1) developing an online-coupling weather and AQPS within the framework of UFS, 2) implementing real-time hourly satellite products to improve representation of wildfire emissions and their impact on air quality predictions, and 3) ensuring the readiness of the online-coupling system for transition to operations. To meet these objectives, a new online-coupling system has integrated the Community Multiscale Air Quality (CMAQ) chemistry component (Byun and Schere, 2006) as a chemistry column model with the Global Forecast System (GFS, NOAA 2023) atmospheric model within the UFS framework. Wildfire emissions are calculated using the Regional Hourly Advanced Baseline Imager (ABI) and Visible Infrared Imaging Radiometer Suite (VIIRS) Emissions (RAVE) data (Li et al., 2022). The

Accepted for publication in *Bulletin of the American Meteorological Society.* DOI 10.1175/BAMS-D-23-0053.1.

UFS-AQM online system was implemented as the operational model (AQMv7) on May 14, 2024, replacing the previous national air quality forecast capability (NAQFC) which was based on the GFS-CMAQ offline system. This paper highlights the scientific advancements and performance improvements of the new online system.

Transition the AQPS to the Unified Forecast System Application

NOAA currently supports more than twenty operational prediction systems, each of which was built with disparate frameworks. To standardize and streamline these systems, NOAA is spearheading an effort to transition most current operational systems to the UFS framework as different applications. The UFS seeks to unify previously disparate modeling systems under a single framework and relies on community support on models and components.

The community modeling system, CMAQ, has been the basis of the operational AQPS at NOAA since the NAQFC was initially deployed in 2004 (Ott et al. 2005; Huang et al., 2016). The previous operational AQPSs were driven by the North American Models (NAMs) and GFS in an offline-coupling mode (Lee et al., 2017; Campbell et al., 2022; Tang et al., 2022).

The next generation regional AQPS is developed by online-coupling CMAQ as a chemistry column model with the UFS-based atmospheric model as one of the regional UFS applications. We describe the configurations of this online-coupling UFS-AQM system with a 13-km grid spacing and present examples of system evaluation.

The Next Generation AQPS in the UFS framework

The UFS-AQM online system: The system comprises several key components: an UFS-based atmospheric model, a National Unified Operational Prediction Capability (NUOPC) layer, the CMAQ chemistry model, emission processing model, and ancillary software for pre- and post-processing. The Geophysical Fluid Dynamics Laboratory (GFDL)'s Finite-Volume Cubed-Sphere (FV3) Dynamical Core (Harris et al., 2021) serves as the engine of the atmospheric model, solving the equations of air motion that describe the behavior of the atmosphere using a finite-volume approach on a cubed-sphere grid (Fig.1).

Accepted for publication in *Bulletin of the American Meteorological Society.* DOI 10.1175/BAMS-D-23-0053.1.

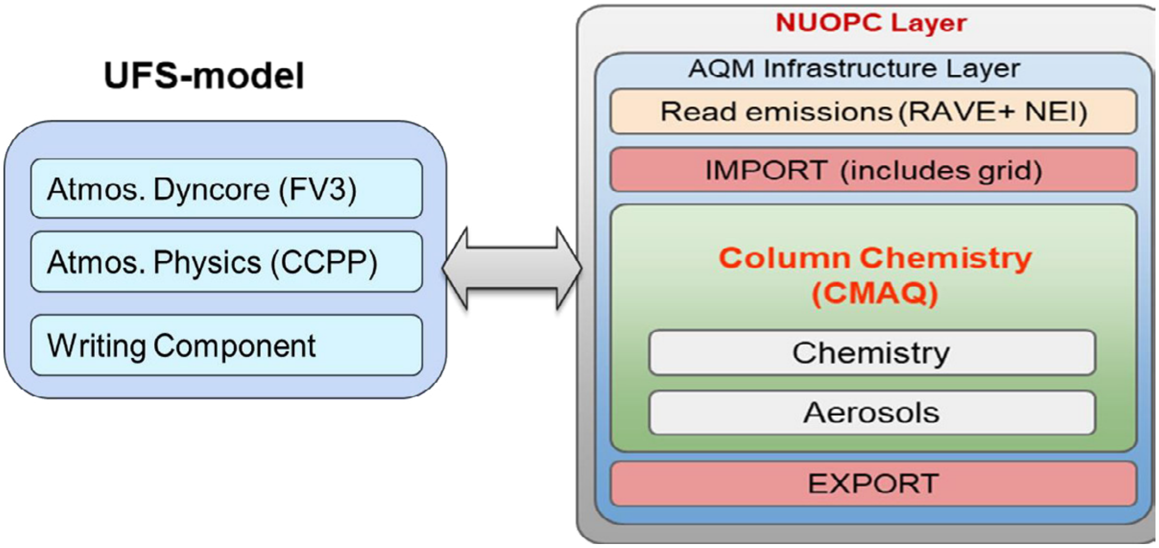

Fig. 1. A framework structure of the UFS-based online air quality prediction system (AQPS).

The Common Community Physics Package (CCPP) provides a framework for implementing physical parameterizations such as radiation, microphysics, boundary layer turbulence, and land surface processes. The CCPP established a standardized set of physical parameterizations that can be used by different modeling groups and applications. The GFS version 16 (v16) physics package (Yang et al., 2020) built within the CCPP is chosen for coupling to the current version of UFS-AQM.

CMAQ is employed by the online system as a column chemistry model to update chemical species concentrations at each integration step. The system disables all transport processes of chemical species within the CMAQ, allowing the FV3 dynamical core to handle the transport of chemical species similar to other physical tracers. The UFS-AQM online system employs the Earth System Modeling Framework (ESMF) library-based NUOPC layer to link the CMAQ atmospheric chemistry column model with the atmospheric model dynamically. At each integration time step, chemical concentrations are communicated between the CMAQ model and the atmospheric model through the NUOPC layer. Both chemical and atmospheric models run on the same horizontal grid and vertical coordinate system, and use the same transport algorithm to ensure consistency between them.

Accepted for publication in *Bulletin of the American Meteorological Society.* DOI 10.1175/BAMS-D-23-0053.1.

The NOAA Emission and Exchange Unified System (NEXUS) is a tool designed to process anthropogenic emission inventories, calculate biogenic emissions, and generate model-grid ready hourly emission rates. It conveniently handles emissions originating from area, mobile, and point sources and generates user-defined model grids ready emission inputs. U.S. EPA National Emission Inventory (NEI) Collaborative provides emission data within the contiguous US (CONUS), while several global emission inventories are integrated to generate emissions for regions outside of the CONUS. The Model of Emissions of Gases and Aerosols from Nature (MEGAN) (Guenther et al., 2023) is incorporated into the NEXUS to calculate biogenic emissions from natural sources. The Fengsha dust module is implemented to replace the default dust module, wind-blown in CMAQ for improving the calculation of real-time dust emissions (Tong et al., 2017).

Real-time hourly RAVE data, derived from multiple satellite active fire products at a spatial resolution of 0.03 degrees, is used to calculate both trace gasses such as carbon monoxide (CO) and nitrogen oxides (NO_x) and $PM_{2.5}$ emissions from wildfires. The new RAVE hourly fire emissions, estimated by fusing high temporal-resolution ABI fire radiative power (FRP) with fine spatial-resolution VIIRS FRP, improve the representation of fire intensity and emission diurnal variation (Li et al., 2022). The plume rise algorithm from Sofiev et al. (2012) is incorporated to effectively distribute both gas and aerosol emissions from wildfires in a vertical manner (Li et al., 2021).

Model configurations: The UFS-AQM online system is tested over a single large North America domain, encompassing three operational domains at a resolution of 13 km (Fig.2), with 65 vertical levels topped at 0.2 hpa. Only results of the CONUS domain are presented in this article. The online system employs the GFSv16 physics package within the CCPP framework, to simulate meteorological fields that drive air quality predictions. The GFSv16 physics package consists of a scale-aware Turbulent Kinetic Energy-based eddy-diffusion mass-flux (TKE-EDMF) Planetary Boundary Layer (PBL) parameterization scheme (Han and Bretherton, 2019), a GFDL six-category cloud microphysics scheme (Chen and Lin, 2013), the simplified Arakawa–Schubert (SAS) shallow and deep cumulus parameterization scheme (Han et al., 2017), and the Noah land surface model (Ek, et al, 2003). Gas-phase chemistry is simulated by using Carbon Bond Mechanism version 6

Accepted for publication in *Bulletin of the American Meteorological Society.* DOI 10.1175/BAMS-D-23-0053.1.

(CB6r3) with updated isoprene chemistry and revised photolysis rates (Yarwood et al., 2010), while aerosol processes are modeled using aerosol module version 6 (AERO6) (Zhang et al., 2018).

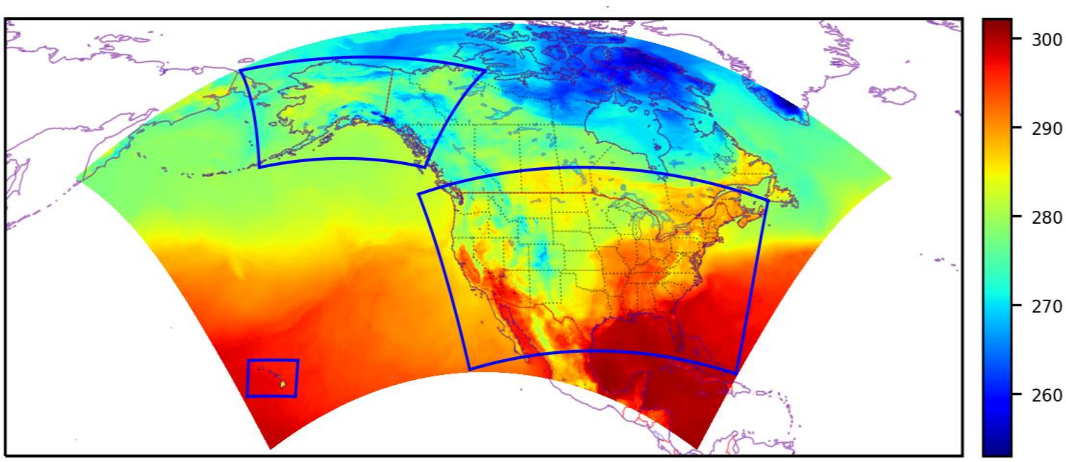

Fig. 2. The North American domain defined by the UFS-AQM online system encompasses three operational product domains: CONUS, Alaska (AK), and Hawaii (HI).

The anthropogenic emission inventories include the 2016 U.S. EPA NEI Collaborative (NEIC) modeling platform (NEIC2016v1) for all gas and aerosol emissions in CONUS (https://www.epa.gov/air-emissions-modeling/2016v1-platform), and a suite of global/mosaic datasets including 1) the combined 2010 Emissions Database for Global Atmospheric Research (EDGAR) (Crippa et al., 2018) - Hemispheric Transport of Air Pollution (HTAP) (Janssens-Maenhout et al., 2015) (EDGAR-for-HTAPv2) for primary $PM_{2.5}$, 2) the 2019 Community Emission Data System Version 2 (CEDSv2) for major gases and primary OC and BC emissions, except for sulfur dioxide (SO_2) that is used only over oceans (Hoesly et al., 2018), and 3) the fused 2019 Ozone Monitoring Instrument (OMI)-HTAP for SO_2 emissions over land areas outside of CONUS.

Hourly real time satellite-retrieved RAVE data, with a grid-spacing of 13-km, is utilized to generate model-grid ready fire emission inputs. $PM_{2.5}$ emission rates are calculated directly from the RAVE product, while emission rates of nitric oxide (NO) and nitrogen dioxide (NO_2) from fires are determined based on the RAVE retrieved CO product following the approach proposed by Campbell et al. (2022). Specifically, we assume that emissions of nitrogen oxides (NO_x) (a sum of NO and NO_2) are equal to 5% of carbon

Accepted for publication in *Bulletin of the American Meteorological Society.* DOI 10.1175/BAMS-D-23-0053.1.

monoxide (CO) emissions, with 90% of this portion attributed to NO. The most recent 24-hr fire emissions are used without any adjustment in the next 72-hr AQ predictions. Volatile organic compounds (VOCs) emissions from wildfires are not incorporated into the online system to improve O_3 over-predictions near wildfire source regions, aligning with the previous operational system (i.e., AQMv6). This warrants an important area for the future development of the UFS-AQM system. Plume rise heights are determined by using FRP. Both gas and aerosol-phase emissions are distributed linearly from the first model level to the top of plume-rise height using the Sofiev scheme.

Monthly-mean lateral boundary conditions (LBCs) for both aerosol composition and gaseous species are generated by utilizing outputs from the GFDL's Atmosphere Model version 4 (AM4) (Horowitz et al., 2020) runs for the year 2019. Real-time Global Ensemble Forecast System (GEFS) aerosol outputs are used to update aerosol species LBCs for the UFS-AQM predictions, following the same approach as the previous operational AQM (i.e., AQMv6). To meet operational product delivery time requirement, previous cycle real-time GFS forecast output files are utilized to generate meteorological initial conditions and LBCs for the current cycle of UFS-AQM runs, and GEFS / aerosol component outputs are used to update the climatological aerosol LBCs dynamically every 6 hours. More details about the UFS-AQM configurations (Dev) proposed to support AQMv7 implementation can be found in Table 1. In addition, the configurations used by the previous operational model, AQM v6, are included for a comparison.

Evaluation of the Model Performance

One of key missions of developing the UFS-based AQM prediction system lies in enhancing the predictability of wildfire air quality. During the early summer of 2023, Canada experienced an extraordinary increase in wildfire activities. These wildfires, coupled with meteorological conditions that promoted the southward movement of wildfire smoke, had a substantial impact on air quality in the US. These events provide a unique opportunity to assess the capabilities of the UFS-AQM prediction system. As an illustrative example, wildfires originating from Quebec, Canada in late June 2023 are

Accepted for publication in *Bulletin of the American Meteorological Society.* DOI 10.1175/BAMS-D-23-0053.1.

spotlighted to demonstrate the online system's efficacy in predicting surface O_3 and $PM_{2.5}$ concentrations.

Table 1. Comparison of model configurations between AQMv6 and UFS-AQM (AQMv7)

	AQMv6	AQMv7
Meteorology and CMAQ	GFSv16/CMAQv5.3.1	UFS-Atmos + CMAQv5.2.1
Gas-phase mechanism/Aerosol module	CB6r3 + Aero7	CB6r3 + Aero6
Anthropogenic emissions	NEIC 2016v1	NEIC 2016v1 for CONUS and CEDS 2019 Global Emissions for O-CONUS
Fire emissions	GBBEPx + Briggs plume rise	RAVE + Sofiev plume rise
CCPP suites	FV3_GFSv16	FV3_GFSv16
Chem-LBCs	GEOS-Chem 2006 + GEFS/Aero	AM4 2019 + GEFS/Aero
Grid spacing and vertical levels	12 km/35 levels	13 km/65 levels

Evaluation of $PM_{2.5}$ predictions near the surface: Smoke produced by wildfires originating from the Province of Quebec, Canada, was transported to the US by following the counter-clockwise wind pattern (Figure S1), significantly affecting air quality across the Midwest to Eastern US. The intrusion started on June 25, 2023, reached the peak severity on June 29, and persisted for approximately one week. Figure 3 presents a comparison of predicted hourly $PM_{2.5}$ concentrations from both AQMv6 and UFS-AQM (AQMv7) against AirNOW observations near ground level on June 28, 2023, across the CONUS domain. AQMv6 denotes the GFS-driven CMAQ offline system, while the AQMv7 represents the UFS-AQM online system. AQMv6 significantly under-predicts $PM_{2.5}$ concentrations over the Great Lakes and surrounding regions, encompassing states such as WI, IL, IN, MI, OH, etc. Notably, the operational predictions fell below 35 μg m^{-3}, whereas the highest recorded observations exceeded 250 μg m^{-3} (Fig. 3a). In contrast, predictions from the UFS-based AQMv7 exhibited much better agreement with observations in terms of magnitude, timing, and spatial distribution (Fig. 3b).

Accepted for publication in *Bulletin of the American Meteorological Society.* DOI 10.1175/BAMS-D-23-0053.1.

Several factors contribute to the significant improvement observed in UFS-AQM predictions. Firstly, AQMv6 relies on daily constant fire emission products (i.e., Global Biomass Burning Emission Product, GBBEPx) with a one-day latency, whereas the UFS-AQM model utilizes real-time satellite active fire products (i.e., RAVE) at an hourly frequency. Secondly, the UFS-AQM runs cover a broad North American domain, effectively capturing air pollutants emitted from fires in the Quebec source region. In contrast, the AQMv6 domain covers CONUS domain only, the fire predictions are constrained by GEFS/Aerosol predictions and influenced by cross-border transport. Thirdly, AQMv6 assumes that a fire persists for 24 hours only for the grid cells with vegetation fraction less than 0.4 over the forest regions in the eastern US (longitude east of 100º W). Fourthly, the consistent physics and transport algorithms, along with the online coupling between the atmosphere and AQ models, provide more accurate meteorological fields that drive AQ predictions with the UFS-AQM system.

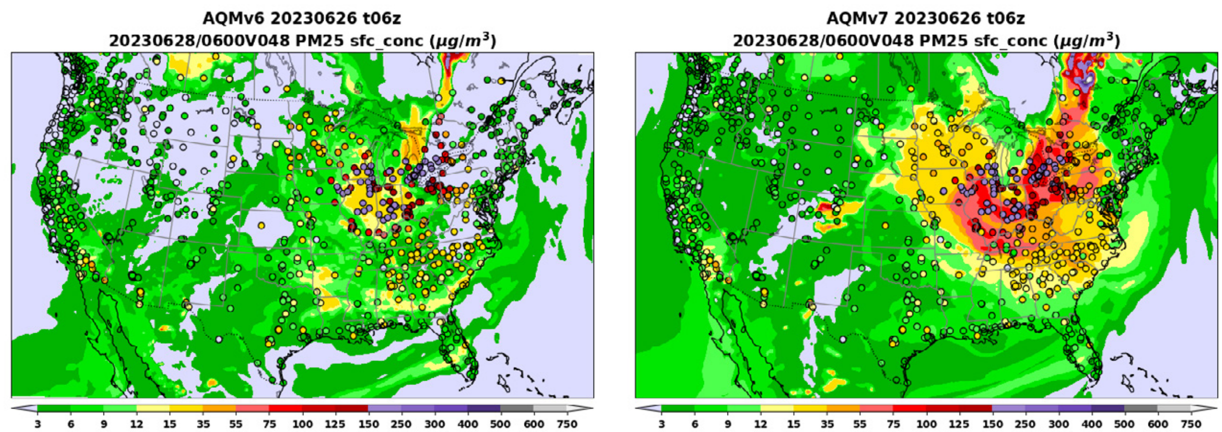

(a) (b)

Fig. 3. A comparison of 24-hour averaged $PM_{2.5}$ predictions between a) AQMv6 (GFS-driven CMAQ offline system) and b) AQMv7 (UFS-AQM online system) along with AirNow observations over the CONUS at 06:00 UTC on June 28, 2023. Model runs were initialized at 06:00 UTC on June 26, 2023) (background: model predictions, circles: AirNow observations).

Figure 4.a further presents a comparison of hourly-averaged $PM_{2.5}$ predictions between AQMv6 and AQMv7 (UFS-AQM) along with AirNow observations averaged over the Eastern US from June 15 to July 15, 2023. The UFS-AQM model accurately captured the peak values (i.e., sub-region average close to 68.0 μg m^{-3}) and temporal patterns of observed $PM_{2.5}$, whereas the operational forecast significantly under-predicted the peak

Accepted for publication in *Bulletin of the American Meteorological Society.* DOI 10.1175/BAMS-D-23-0053.1.

values, partially attributed to its omission of wildfire emissions over eastern US (Campbell, et al., 2022). Figure 4.b compares the categorical performance between the two prediction systems on hourly-averaged $PM_{2.5}$ predictions across the Eastern US. The comparison employs three statistical parameters, evaluated at ten different thresholds values (5, 10, 12, 15, 20, 25, 35, 45, 55, and 65 $\mu g \cdot m^{-3}$): success ratio (1-FAR, where FAR denotes false alarm rate), probability of detection (POD), and critical success index (CSI). Higher CSI values indicates superior performance. The ideal scenario will be at the right top corner of the diagram. The UFS-AQM consistently demonstrates higher values of CSI across all the thresholds, indicating its superior performance compared to AQMv6, particularly during the intense wildfire events. Similar plots for the Western US can be found in Figure S2 for reference.

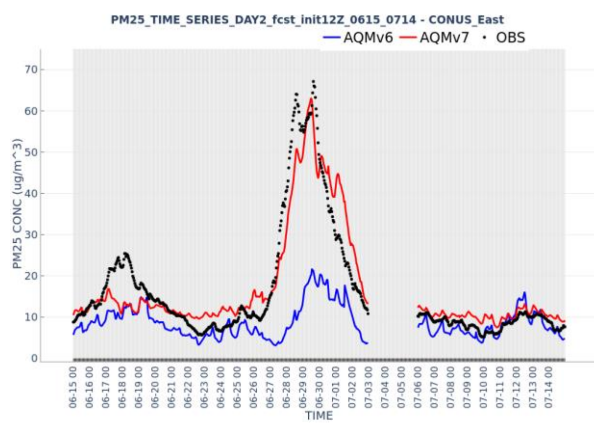

(a)

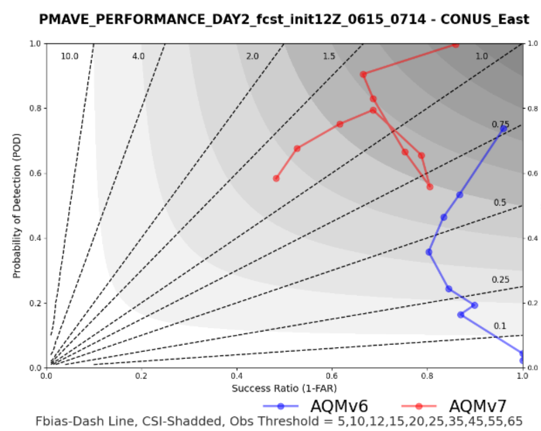

(b)

Fig. 4. a) A time series comparison of hourly-averaged $PM_{2.5}$ concentrations between the previous operational model (AQMv6, blue) and the UFS-AQM model (AQMv7, red) and AirNow observations (black) (Note: the discontinuity in the the time series is due to the exclusion of high $PM_{2.5}$ caused by firework emissions); b) Performance diagram of 24-hr average $PM_{2.5}$ predictions between AQMv6 (blue) and AQMv7 (red) at threshold values of 5, 10, 12, 15, 20, 25, 35, 45, 55, and 65 $\mu g \cdot m^{-3}$ over the Eastern US from June 15th to July 14th, 2023.

Evaluation of O_3 predictions: Wildfires emit not only aerosols but also gas species such as CO, NO_x, and VOCs. Among these gas species, NO_x and VOCs act as primary precursors for O_3 formation in the lower troposphere. Typically, regions proximate to wildfire sources exhibited diminished O_3 formation due to substantial attenuation of the aerosol radiative effect. Consequently, O_3 concentrations tend to be low in these areas.

Accepted for publication in *Bulletin of the American Meteorological Society.* DOI 10.1175/BAMS-D-23-0053.1.

Conversely, downstream regions experienced a significant increase in ambient O_3 levels, especially during the dissipation stage of wildfires. For instance, several instances of O_3 exceedance were observed over the Eastern US coastal region on June 29-30, July 1, 2023 when Quebec fire impact experienced the latest stage over the US. Fig. 5a illustrates the daily maximum 8-hour average O_3 concentrations over the Northeastern US on June 30, 2023. O_3 concentrations exceeded the US EPA National Ambient Air Quality Standard (NAAQS) for the daily maximum 8-hour average O_3 (set at 70.0 ppbv) at many sites in Northeastern Coastal regions, including New York, New Jersey, and Pennsylvania.

During this event, AQMv6 significantly under-predicted the O_3 exceedance, whereas the UFS-AQM model accurately captured the O_3 exceedance events at those downstream locations due to much higher precursor emissions transported from the wildfire source regions in the UFS-AQM. However, it's worth noting that the UFS-AQM

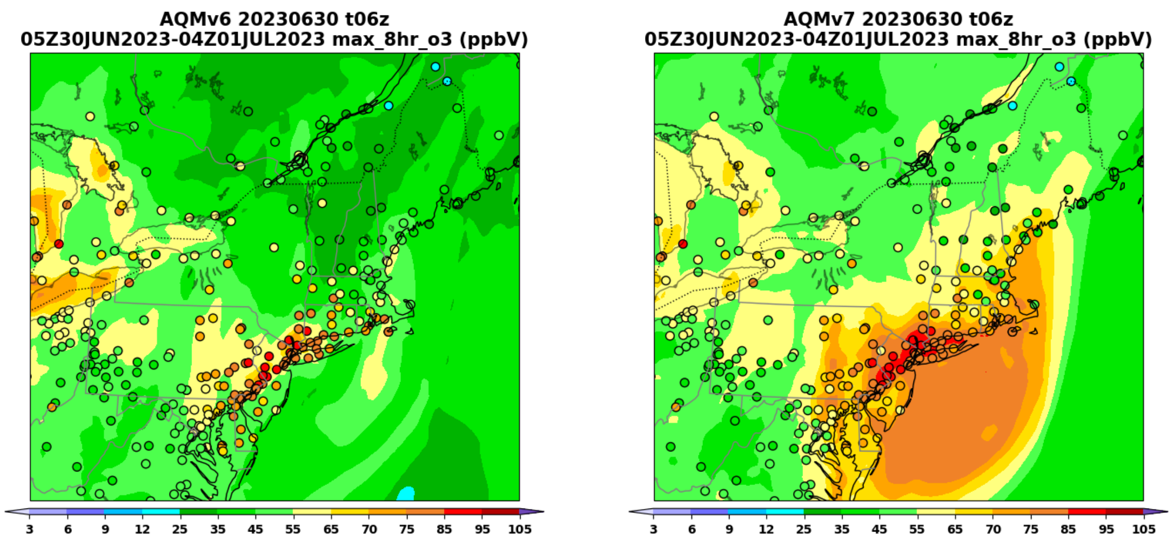

(b)

(a)

Fig. 5. A comparison of daily maximum 8-hour average O_3 predictions between a) AQMv6 (GFS-driven CMAQ offline system) and b) AQMv7 (UFS-AQM online system) along with AirNow observations over the Northeastern US on June 30th, 2023. Model runs were initialized at 06:00 UTC on June 29, 2023) (background: model predictions, circles: AirNow observations).

model also displayed elevated false alarm rates in several states in the Northeastern US, including CT, MA, and RI, etc.

Accepted for publication in *Bulletin of the American Meteorological Society.* DOI 10.1175/BAMS-D-23-0053.1.

A time series comparison of daily maximum 8-hour average O_3 between two prediction systems together with AirNow observations is presented in Fig.6a. Consistent with spatial distributions, the UFS-AQM predicted higher O_3 concentrations, which are closer to the

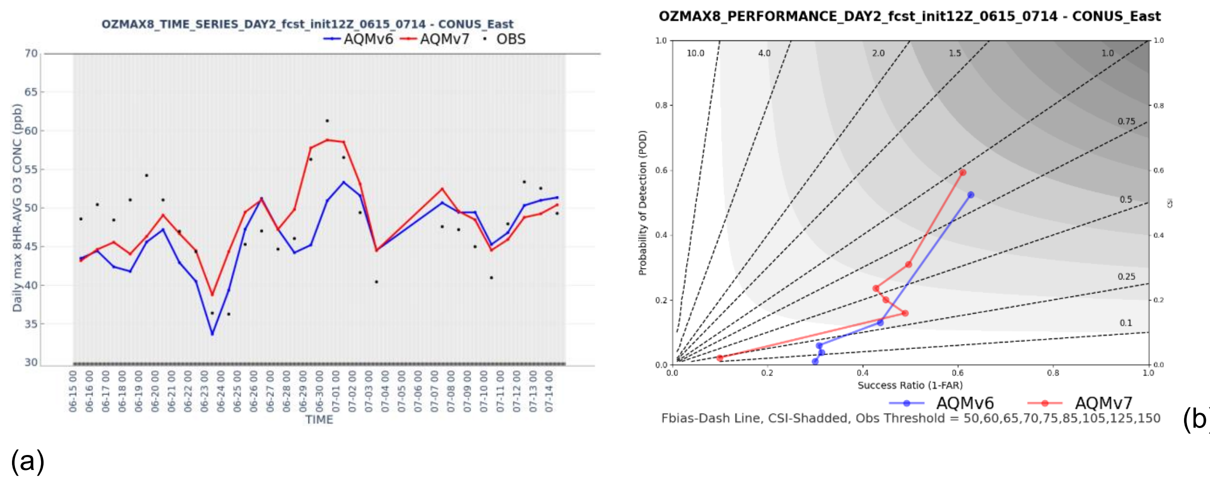

Fig. 6. a) A time series comparison of daily maximum 8-hour average O_3 and b) performance diagram of daily maximum 8-hour average O_3 at threshold values of 50, 60, 65, 70, 75, 85, 105, 125, and 150 ppb over the Eastern US from June 15 to July 14, 2023.

observations compared to the previous operational forecasts for the most days during the study period. The performance diagram (Fig.6b) further demonstrates the UFS-AQM online system's superior predictive performance in terms of both CSI and POD values for daily maximum 8-hour average O_3. For some cases, higher POD is accompanied by higher false alarm rates in predicting O_3 exceedance events.

Comparison of model-predicted aerosol optical depth (AOD) with satellite retrieval data: We expand our model performance evaluation from the near-surface to vertical columns, specifically assessing the model's ability to predict AOD. In Fig. 7, we present a comparison of the simulated AOD from the previous operational model (AQMv6) and the UFS-AQM system (AQMv7) with AOD data retrieved from VIIRS at 19z UTC on June 27, 2023. The previous operational model significantly under-predicts AOD with values less than 1.5 (Fig. 7a). In contrast, the UFS-AQM system accurately predicts the spatial distribution of AOD, with values exceeding 3.5 observed over the Great Lakes and surrounding areas (Fig.7b). These spatial patterns align closely with the near-surface $PM_{2.5}$ predictions. This alignment further demonstrates the UFS-AQM system's capacity

Accepted for publication in *Bulletin of the American Meteorological Society.* DOI 10.1175/BAMS-D-23-0053.1.

of predicting wildfire events for both surface concentrations and vertically integrated mass.

Overall, the enhanced predictive capabilities of the UFS-AQM model primarily stem from two crucial factors. Firstly, the integration of a real-time satellite-derived high spatio-temporal resolution wildfire product RAVE, ensures a more precise representation of wildfire emissions. Secondly, the online coupling of atmospheric and chemistry models leads to more frequent updates of meteorological inputs in the AQM (i.e., CMAQ column model). This dual enhancement approach not only refines the representation of emissions but also maintains a more dynamic and updated predictions of atmospheric fields that govern chemical reactions and transport of chemical species in the AQM.

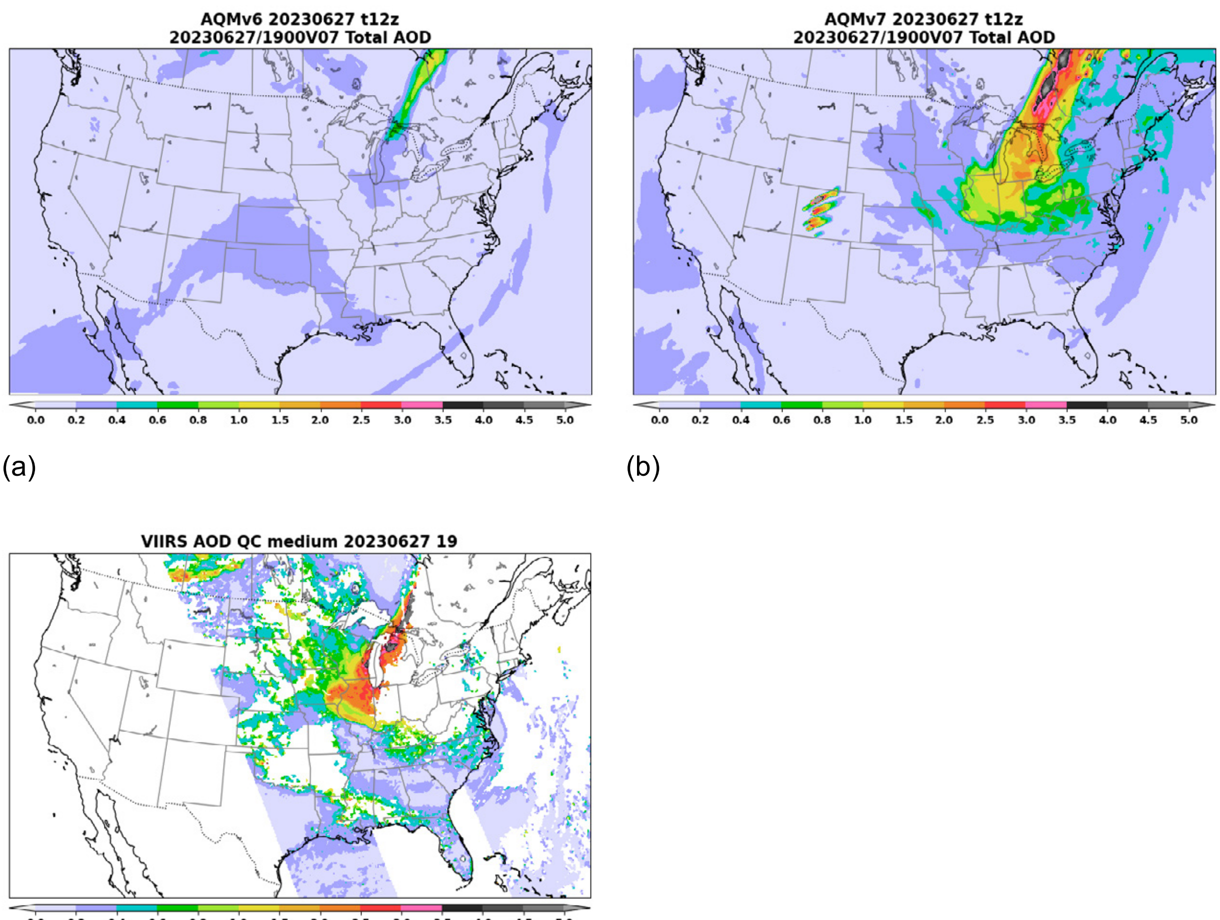

(a) (b)

(c)

Accepted for publication in *Bulletin of the American Meteorological Society.* DOI 10.1175/BAMS-D-23-0053.1.

Fig. 7. a) Previous operational model (AQMv6) predicted aerosol optical depth (AOD), b) UFS-AQM-predicted AOD, and c) Visible Infrared Imaging Radiometer Suite (VIIRS)-retrieved AOD at 19z UTC on June 27, 2023.

Summary

NOAA has developed an advanced regional AQM prediction system within the UFS framework, aiming to improve the accuracy of air quality predictions for the US, particularly during wildfire events. This system employs dynamic coupling between the UFS-based atmospheric model and EPA's CMAQ modeling system, being treated as a column atmospheric chemistry model. This online coupling approach provides more frequent and precise meteorological inputs, mitigating uncertainties associated with grid-mapping and vertical interpolation in offline coupling. As a result, this approach improves wildfire and air quality predictions.

To enhance the representation of wildfire emissions, the online system utilizes data from the NESDIS RAVE product, offering improved source location, intensity, duration, plume-rise height, and vertical distribution information. The online system was implemented as an operational air quality prediction system (AQMv7) on May 14, 2024, replacing the GFS-CMAQ offline system (AQMv6).

A recent wildfire event originating from Quebec Province, Canada, is selected to illustrate the superior capabilities of the UFS-AQM online prediction system. The UFS-AQM predictions are compared with the previous operational forecast and evaluated against AirNow observations. The results demonstrate significant improvement in $PM_{2.5}$ prediction accuracy in terms of both magnitude and spatial distribution patterns during the Quebec wildfire in late June 2023, compared to the operational system. Meanwhile, the UFS-AQM outperforms in predicting O_3 exceedance events, particularly in Northeastern US coastal regions, as indicated by higher CSI and POD values, although it occasionally exhibits higher false alarm rates. Moreover, a comparison was conducted between the model-predicted AOD and VIIRS retrieval data, demonstrating the UFS-AQM's proficiency in predicting surface $PM_{2.5}$ and vertically integrated aerosol mass.

Accepted for publication in *Bulletin of the American Meteorological Society.* DOI 10.1175/BAMS-D-23-0053.1.

The UFS-AQM online system has consistently demonstrated improved performance in predicting the heavy wildfire events such as the one occurring in the Northwestern coastal regions of US in September 2020 and several others heavy wildfire events originated from Canada in summer 2023. The results of more comprehensive evaluation for those time periods will be presented in a separate publication, along with the analysis of bias-corrected forecast products.

Efforts to assimilate surface $PM_{2.5}$ observations and satellite retrievals of AOD and NO_2 to improve the initialization of chemical fields are underway. Some possible future development may include improved representation of emissions, such as volatile organic compounds from wildfires. Development may proceed to refine model resolution to address air quality prediction challenges over complex terrains and coastal regions. This may include machine-learning emulators to improve computational efficiency for chemical reactions and dynamical transport within the system.

Acknowledgement. Development of AQMv7 has been funded by supplemental funding through H.R.2157 - Additional Supplemental Appropriations for Disaster Relief Act, 2019,

Disaster Relief Supplemental Appropriations Act 2022, and OSTI NAQFC program. The authors thank Chuanyu Xu from I.M. Systems Group, Inc. at NOAA/NESDIS for processing the RAVE data, and Li Pan from Lynker at NOAA/NWS/NCEP/EMC for providing GEFS/Aerosol outputs.

Statement on Model and Data Availability: The UFS-AQM package is available for access and download on the following GitHub repository: GitHub Link. Operational forecast productions can be obtained from https://www.nco.ncep.noaa.gov/pmb/products/aqm. However, the UFS-AQM predictions data featured in the study will be provided upon request from interested readers.

Disclaimer: The scientific results and conclusions, as well as any views or opinions expressed herein, are those of the authors and do not necessarily reflect the views of NOAA or the Department of Commerce.

Accepted for publication in *Bulletin of the American Meteorological Society.* DOI 10.1175/BAMS-D-23-0053.1.

References

Andreae, M. O., 2019: Emission of trace gases and aerosols from biomass burning – an updated assessment. A*tmos. Chem. Phys*., 19, 8523–8546, https://doi.org/10.5194/acp-19-8523-2019.

Bellasio, R., and K. M. Foley, 2016: A review of the application of commonly used atmospheric models for particulate matter modeling: focus on dispersion model performance. *Atmos. Pollut. Res.,* 7(4), 579-594.

Bowman, D. M. J. S., C. A. Kolden, J. T. Abatzoglou, et al., 2020: Vegetation fires in the Anthropocene. *Nat. Rev. Earth Environ*. **1**, 500-515.

Burke, M., A., Driscoll, S. Heft-Neal, J. Xue, J. Burney, and M. Wara, 2021: The changing risk and burden of wildfire in the United States. *Proc., Natl., Acad., Sci*., **118**, e2011048118.

Byun, D. W. and K. L. Schere, 2006: Review of the governing equations, computational algorithms, and other components of the Models-3 Community Multiscale Air Quality (CMAQ) modeling system. *Appl. Mech. Rev.*, 59(2), 51-77.

Campbell, P. C., Y. Tang, P. Lee, et al., 2022: Development and evaluation of an advanced National Air Quality Forecasting Capability using the NOAA Global Forecast System version 16. *Geosci. Model Dev.*, 15, 3281–3313, 2022 https://doi.org/10.5194/gmd-15-3281-2022.

Chatfield, R. B., M. O. Andreae, ARCTAS Science Team, and SEAC4RS Science Team, 2020: Emissions relationships in western forest fire plumes – Part 1: Reducing the effect of mixing errors on emission factors. *Atmos. Meas. Tech.*, 13, 7069–7096, https://doi.org/10.5194/amt-13-7069-2020.

Chen, J. -H. and S. J., Lin, 2013: Seasonal predictions of tropical cyclones using a 25 km-resolution general circulation model, *J. Climate*, 26, 380–398, https://doi.org/10.1175/JCLI-D-12-00061.1.

Crippa, M., D. Guizzardi, M. Muntean, E. Schaaf, F. Dentener, J. A. van Aardenne, S. Monni, U. Doering, J. G. J. Olivier, V. Pagliari, and G. Janssens-Maenhout, 2018: Gridded

Accepted for publication in *Bulletin of the American Meteorological Society.* DOI 10.1175/BAMS-D-23-0053.1.

emissions of air pollutants for the period 1970–2012 within EDGAR v4.3.2. *Earth Syst. Sci. Data*, 10(4), 1987-2013.

Demetriou, C. A. and Vineis, P., 2015: Carcinogenicity of ambient air pollution: use of biomarkers, lessons learnt and future directions. *J. Thorac. Dis.*, 7, 67–95, https://doi.org/10.3978/j.issn.2072- 1439.2014.12.31.

Ek, M. B., K. E. Mitchell, Y. Lin, E. Rogers, P. Grunmann, V. Koren, G. Gayno, and J. D. Tarpley, 2003: Implementation of Noah land surface model advances in the National Centers for Environmental Prediction operational mesoscale Eta model. *J. Geophys. Res.*,108(D22), 8851, doi:10.1029/2002JD003296.

Fann, N., A. D. Lamson, S. C. Anenberg, K. Wesson, D. Risley, and B. J. Hubbell, 2012: Estimating the national public health burden associated with exposure to ambient PM2.5 and ozone. *Risk Anal.*, 32(1), 81-95. https://doi.org/10.1111/j.1539-6924.2011.01630.x.

Guenther, A. B., Jiang, X., Heald, C. L., Sakulyanontvittaya, T., Duhl, T., Emmons, L. K., and Wang, X., 2012: The Model of Emissions of Gases and Aerosols from Nature version 2.1 (MEGAN2.1): an extended and updated framework for modeling biogenic emissions. *Geosci. Model Dev.,* **5**, 1471–1492, https://doi.org/10.5194/gmd-5-1471-2012.

Han, J. and C. S., Bretherton, 2019: TKE-Based Moist EddyDiffusivity Mass-Flux (EDMF) Parameterization for Vertical Turbulent Mixing. *Weather Forecast*., **34**, 869–886, https://doi.org/10.1175/WAF-D-17-0046.1.

Han, J., Wang, W., Kwon, Y. C., Hong, S.-Y., Tallapragada, V., and Yang, F., 2017: Updates in the NCEP GFS Cumulus Convection Schemes with Scale and Aerosol Awareness. *Weather Forecast.*, **32**, 2005–2017, https://doi.org/10.1175/WAF-D-17-0046.1.

Harris, L., X. Chen ; W. Putman, L. Zhou, J. Chen, 2021; A Scientific Description of the GFDL Finite-Volume Cubed-Sphere Dynamical Core. *NOAA technical memorandum OAR GFDL*; 2021-001, DOI : https://doi.org/10.25923/6nhs-5897.

Hoesly, R. M., Smith, S. J., Feng, L., Klimont, Z., Janssens-Maenhout, G., Pitkanen, T., Seibert, J. J., Vu, L., Andres, R. J., Bolt, R. M., Bond, T. C., Dawidowski, L., Kholod, N.,

Accepted for publication in *Bulletin of the American Meteorological Society.* DOI 10.1175/BAMS-D-23-0053.1.

Kurokawa, J.-I., Li, M., Liu, L., Lu, Z., Moura, M. C. P., O'Rourke, P. R., and Zhang, Q., 2018: Historical (1750–2014) anthropogenic emissions of reactive gases and aerosols from the Community Emissions Data System (CEDS). *Geosci. Model Dev.*, **11**, 369–408, https://doi.org/10.5194/gmd-11-369-2018.

Horowitz, L. W., V. Nail, F. Paulo, et al., 2020: The GFDL Global Atmospheric Chemistry-Climate Model AM4.1: Model Description and Simulation Characteristics, *J. Adv. Model Earth System*, 2, e2019MS002032. https://doi.org/10.1029/2019MS002032.

Jacobs, N. A., 2021: Open Innovation and the Case for Community Model Development. *B. Am. Meteorol. Soc.*, 102(10), E2002-E2011, https://doi.org/10.1175/BAMS-D-21-0030.1

Janssens-Maenhout, G., M. Crippa, D. Guizzardi, F. Dentener, M. Muntean, G. Pouliot, T. Keating, Q. Zhang, J. Kurokawa, R. Wankmüller, H. Denier van der Gon, J. J. P. Kuenen, Z. Klimont, G. Frost, S. Darras, B. Koffi, and M. Li, 2015: HTAP_v2.2: a mosaic of regional and global emission grid maps for 2008 and 2010 to study hemispheric transport of air pollution. *Atmos. Chem. Phys.*, 15, 11411–11432, https://doi.org/10.5194/acp-15-11411-2015.

Johnston, F. H., S. B. Henderson, Y. Chen, J. T. Randerson, M. Marlier, et al., Estimated global mortality attributable to smoke from landscape fires. *Environ. Health Perspect.* **120**, 695-701.

Kar Kurt, O., J. Zhang, and K. E. Pinkerton, 2016: Pulmonary Health Effects of Air Pollution, *Curr. Opin. Pulm. Med.*, 22, 138–143, https://doi.org/10.1097/MCP.0000000000000248.

Lee, P., J. McQueen, I. Stajner, J. Huang, L. Pan, D. Tong, H. Kim, Y. Tang, S. Kondragunta, M. Ruminski, S. Lu, E. Rogers, R. Saylor, P. Shafran, H. C. Huang, J. Gorline, S. Upadhayay, and R. Artz, 2017: NAQFC Developmental Forecast Guidance for Fine Particulate Matter (PM2.5). *Weather Forecast.,* 32, 343–360, https://doi.org/10.1175/waf-d-15-0163.1

Li, Y., D. Tong, S. Ma, X. Zhang, S. Kondragunta, F. Li, and R. Saylor, 2021: Dominance of wildfires impact on air quality exceedances during the 2020 record-breaking wildfire

Accepted for publication in *Bulletin of the American Meteorological Society.* DOI 10.1175/BAMS-D-23-0053.1.

season in the United States. *Geophys. Res. Lett.*, 48, e2021GL094908. https://doi.org/10.1029/2021GL094908,.

Li, F., X. Y. Zhang, S. Kondragunta, X. Lu, I. Csiszar, and C. C. Schmidt, 2022: Hourly biomass burning emissions product from blended geostationary and polar-orbiting satellites for air quality forecasting applications. *Remote Sens. Environ.*, **281**, 113237, https://doi.org/10.1016/j.rse.2022.113237.

NOAA, 2023: An overview of development and implementation of the global forecast system at NOAA, https://www.emc.ncep.noaa.gov/emc/pages/numerical_forecast_systems/gfs.php (last access on May 5, 2024).

Schill, G. P., K. D. Froyd, H. Bian, A. Kupc, C. Williamson, et al., 2020: Widespread biomass burning smoke throughout the remote troposphere. *Nat. Geosci.* **13**, 422-427.

Sofiev, M., T. Ermakova, and R. Vankevich, 2012: Evaluation of the smoke-injection height from wild-land fires using remote-sensing data. *Atmos. Chem. Phys*., **12**, 1995–2006, https://doi.org/10.5194/acp-12-1995-2012.

Tang, Y., P. C. Campbell, P. Lee, et al., 2022: Evaluation of the NAQFC driven by the NOAA Global Forecast System (version 16): comparison with the WRF-CMAQ during the summer 2019 FIREX-AQ campaign. *Geosci. Model Dev*., **15**, 7977–7999, https://doi.org/10.5194/gmd-15-7977-2022.

Tong, D. Q., Wang, J. X. L., Gill, T. E., Lei, H., and Wang, B., 2017: Intensified dust storm activity and Valley fever infection in the southwestern United States. *Geophys. Res. Lett.,* 44, 4304–4312, https://doi.org/10.1002/2017GL073524.

US Environmental Protection Agency, Data from the 2017: National Emissions Inventory (2017). https://www.epa.gov/air-emissions-inventories/2017-national-emissions-inventory-nei-data (last accessed May 5, 2024).

Xie, Y., M. Lin, B. Decharme, C. Delire, L. Horowitz, D. M. Lawrence, F. Li, and R. Séférian, 2022: Tripling of western US particulate pollution from wildfires in a warming climate. *PNAS*, **119**, https://doi.org/10.1073/pnas.2111372119.

Accepted for publication in *Bulletin of the American Meteorological Society.* DOI 10.1175/BAMS-D-23-0053.1.

Yang, F., T. Vijay, J. Kain, H. Wei, R. Yang, V Yudin, S. Moorthi, J. Han, Y. Hou, J. Wang, R. Treadon, and D. T. Kleist, 2020: Model Upgrade Plan and Initial Results from a Prototype NCEP Global Forecast System Version 16, 100th AMS Annual Meeting 12–16 January 2020, Boston.

Yarwood, G., J. Jung, G. Z. Whitten, G. Heo, J. Mellerg, and M. Estes, 2010: Updates to the Carbon Bond Mechanism for Version 6, the 9th Annual CMAS Conference, Chapel Hill, NC, October 11-13, 2010. Available online at Here (last access: May 5, 2024).

Zhang, H., L. D. Yee, B. H. Curtis, M. P. Worton, et al., 2018: Monoterpenes are the largest source of summertime organic aerosol in the southeastern United States, *Proc. Natl. Acad. Sci.,* **115**, 2038- 2043, doi.org/10.1073/pnas.1717513115.

Accepted for publication in *Bulletin of the American Meteorological Society.* DOI 10.1175/BAMS-D-23-0053.1.